

## First-principles study of the electronic and optical properties of confined silicon systems

Sun-Ghil Lee, Byoung-Ho Cheong, Keun-Ho Lee, and K. J. Chang

*Department of Physics, Korea Advanced Institute of Science and Technology, 373-1 Kusung-dong, Yuseong-ku, Daejeon, Korea*

(Received 29 June 1994; revised manuscript received 1 September 1994)

We examine the band structure and the dielectric response of confined Si systems such as quantum wells and wires through first-principles pseudopotential calculations and find the direct band gaps. With the surfaces of the quantum systems saturated by hydrogen atoms, the optical excitation peaks in the range of visible light are prominent, as compared to those with unsaturated Si dangling bonds. In quantum wires, we find luminescence excitation peaks near the band-gap energy, in good agreement with measured absorption spectra. At energies higher by about 1 eV than the band-edge excitation spectra, we also find strong wire-related absorption peaks, while these were previously interpreted as bulklike excitations. We analyze optical absorption spectra and find strong transitions between relatively localized states that are caused by strong Si-H bonds and quantum confinement in the near-surface region. In correlating to the photoluminescence in porous Si, the importance of quantum confinement and surface effects is stressed.

One of the shortcomings of crystalline Si is weak band-edge luminescence due to the indirect band gap; thus its applications for optical devices have been limited. Many efforts have been made to increase luminescence efficiency from Si. Recently, highly efficient visible luminescence was observed in passivated Si crystallites with diameters in the range 20–50 Å.<sup>1</sup> The sizes of Si quantum systems produced by the anodization of Si wafers at low current densities in HF-based solutions were shown to depend on anodization conditions and substrate resistivity.<sup>1</sup> Because of the small size of the system, the quantum confinement effect was suggested to be the origin of photoluminescence from porous Si.<sup>1</sup> It was shown that the photoluminescence peak increases as the porosity of a sample increases.<sup>1</sup> There have been numerous experimental<sup>2–5</sup> and theoretical works<sup>6–9</sup> which support such an idea. Since porous Si can be viewed as a collection of quantum wires, the hydrogen or siloxene adsorbed on rich surfaces may play an important role in luminescence. Despite some emphasis on the role of oxides at surfaces,<sup>3,10</sup> oxidation was shown to cause degradation of luminescence.<sup>11,12</sup> On the other hand, the formation of silicon hydrides at surfaces was suggested to be a possible origin of luminescence because the chemical etching in HF solutions is a necessary and crucial process in obtaining efficient luminescence.<sup>13–15</sup>

In this work we perform self-consistent *ab initio* pseudopotential calculations to study the electronic and optical properties of Si quantum systems. Considering quantum wells and wires with surfaces saturated by hydrogen, we calculate the dielectric response functions and find strong optical excitation peaks in the visible light region for both the systems. These quantum systems are characterized by some localized states which are produced by quantum confinement and strong interactions between hydrogen and surface Si atoms, exhibiting strong optical transitions between these states. We compare the band structures and the dielectric functions for the confined systems with those for free Si surfaces and emphasize

the role of hydrogen in luminescence from porous Si. We also find anisotropic behavior in the optical absorption of the quantum systems.

Our calculations are based on the first-principles pseudopotential method<sup>16</sup> within the local-density functional approximation (LDA).<sup>17</sup> The Wigner interpolation formula is used for the exchange and correlation potential.<sup>18</sup> Norm-conserving nonlocal pseudopotentials are generated by the scheme of Troullier and Martins,<sup>19</sup> then they are transformed into the separable form of Kleinman and Bylander.<sup>20</sup> A plane wave basis set is used to expand the wave functions with a kinetic energy cutoff of 10 Ry. The total energy is fully minimized by the modified Jacobi relaxation method which was recently developed and employed successfully for a variety of systems.<sup>21</sup> In our calculations, we chose two quantum wells (see Fig. 1), the supercells of which consist of five and nine Si layers and 5–6 vacuum layers along the [001] direction, respectively. In the quantum wire, we employ an array of Si wires which are similar to those used in previous calculations.<sup>6–8</sup> The Si wires are aligned along the [001] direction with a supercell containing 25 Si atoms (denoted by a 5×5 quantum wire because the cubic cross section has five Si layers on both the axes). We also test a larger quantum wire which has 49 Si atoms in a unit cell (denoted by a 7×7 quantum wire). The separations between Si quantum wires are 15.36 and 19.20 Å for the 5×5 and 7×7 wires, respectively. For all the quantum structures, the dangling bonds at the surfaces are passivated by hydrogen atoms. To examine absorption and photoluminescence excitation spectra, we calculate the imaginary part of the dielectric function in the optical limit  $\mathbf{q} \rightarrow 0$ :

$$\epsilon_2(\omega) = \frac{4\pi^2 e^2}{m_e^2 \omega^2} \sum_{v,c} \int_{\text{BZ}} \frac{2d\mathbf{k}}{(2\pi)^3} |\langle \psi_{c,\mathbf{k}} | \mathbf{e} \cdot \mathbf{p} | \psi_{v,\mathbf{k}} \rangle|^2 \times \delta[E_c(\mathbf{k}) - E_v(\mathbf{k}) - \hbar\omega], \quad (1)$$

where  $E_c$  and  $E_v$  denote the energies of the conduction

$(\psi_{c,\mathbf{k}})$  and valence band  $(\psi_{v,\mathbf{k}})$  states, respectively, at a  $\mathbf{k}$  point,  $\mathbf{e}$  is the polarization vector of an external field,  $\mathbf{p}$  is the momentum operator,  $m_e$  is the free-electron mass, and  $\hbar\omega$  is the photon energy. In the band summation, sufficient conduction band states are included so that the energy in the dielectric function is expanded up to about 10 eV. The linear tetrahedron method is employed to perform the summation over the Brillouin zone (BZ).<sup>22</sup> In the quantum wells, 360  $\mathbf{k}$  points in the irreducible BZ are chosen while 72 and 42  $\mathbf{k}$  points are used in the  $5\times 5$  and  $7\times 7$  quantum wires, respectively.

The calculated band structures for the quantum well and wire are drawn in Fig. 2. It is clearly seen that the

band gaps are direct at the  $\Gamma$  point, while bulk Si has an indirect band gap. The conduction band minimum (CBM) states, which are denoted by  $C_1$  and  $C_m$  for the quantum well and wire, respectively, at the  $\Gamma$  points are derived by the band folding effect from the  $X$  state of bulk Si. If the CBM states have the same symmetry as that of the  $X$  state, the optical transitions from the valence band maximum (VBM) to these CBM states will be forbidden as in bulk crystalline Si. We first examine the optical properties of the quantum well and wire by calculating the oscillator strength:

$$f_{c,v} = \frac{2}{m_e \Delta E} |\langle \psi_{c,\mathbf{k}} | \mathbf{e} \cdot \mathbf{p} | \psi_{v,\mathbf{k}} \rangle|^2, \quad (2)$$

where  $\Delta E$  is the energy difference between the conduction and valence band states. In both the quantum well and wire, the calculated oscillator strengths are listed and compared in Table I. We find strong oscillator strengths for the optical transitions between the states near the conduction and valence band edges. In the five-layer quantum well, the oscillator strength is found to be strongest for the transition from the  $V_1$  VBM state to the  $C_3$  conduction band state, while the oscillator strengths are about two times smaller for the transitions from the  $V_4$  state to the  $C_1$  and  $C_3$  conduction band states. In the case of the  $5\times 5$  quantum wire, strong oscillator strengths are found for the  $V_m-C_s$  and  $V_m-C_b$  transitions. Since the  $C_1$  and  $C_m$  states correspond to the CBM states of the quantum systems, the optical transition from the VBM state to the CBM state is found to be extremely weak as in bulk Si. However, the transition from the  $V_4$  state to the CBM state exhibits fairly strong oscillator strength in both the quantum systems.

To investigate the electronic origin of the  $C_3$  state which lies at about 1 eV above the CBM state, we consider two different quantum wells; in one case, all the dangling bonds at surfaces remain nonpassivated and in the other case one-half of the dangling bonds are passivated by hydrogen atoms. We compare their band structures with that of *c*-Si in Fig. 3. We find that the  $C_1$  and  $C_5$  states in the quantum well band structure also appear in the conduction bands of bulk Si; thus these states are little affected by either the quantum confinement or hydrogenation effects. However, the  $C_3$  state is only seen in the quantum well structure, independently of the degree of hydrogenation at the surfaces. Thus this state is derived from the quantum confinement effect rather than H bonding at the surfaces. Similar behavior is also found for the  $C_s$  state in the quantum wire. Although the electronic states in *c*-Si are normally extended over space, fairly localized states are expected in the quantum systems because of the abrupt potential changes in the surface region. The electronic charge densities for the  $C_3$  state of the quantum well and the  $C_s$  state of the quantum wire are drawn in Fig. 4. Both the charge densities are mostly accumulated between the surface Si layer and its sublayer, reflecting that they are surface-related states. On the other hand, we find that the  $V_1$  state in the quantum well is associated with the Si-H bonds at the surfaces. As illustrated in Fig. 4, the electronic charge densities are largely filled up in the bonding region

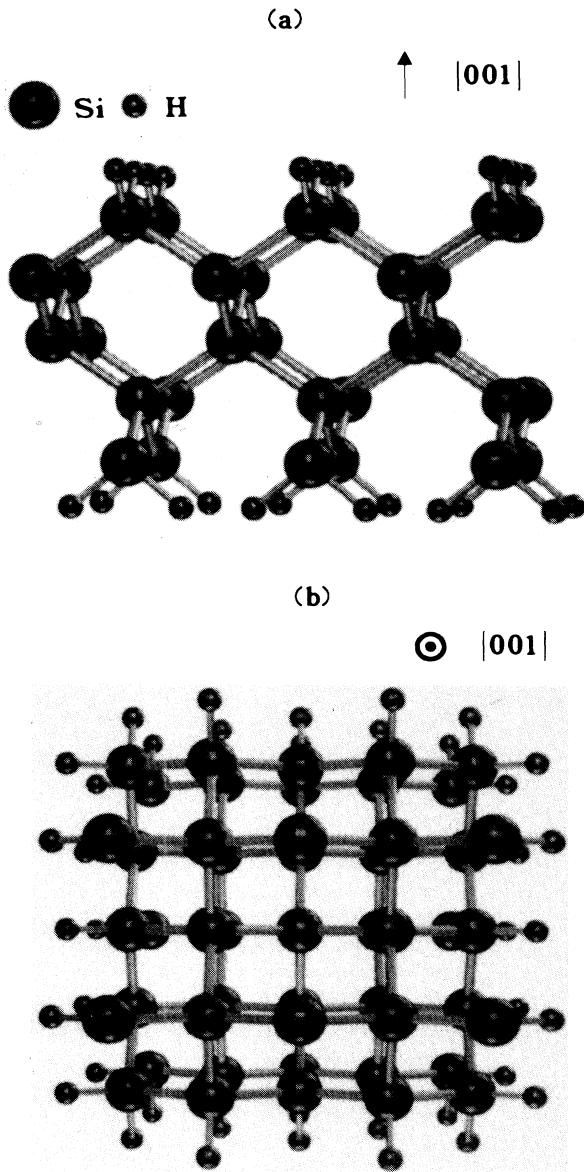


FIG. 1. Ball and stick models for the five-layer quantum well (a) and  $5\times 5$  quantum wire (b). The unit cell of the quantum well includes five Si and four H atoms and is repeated on the  $(001)$  plane. The wire is chosen along the  $[001]$  direction with the unit cell containing 25 Si and 20 H atoms.

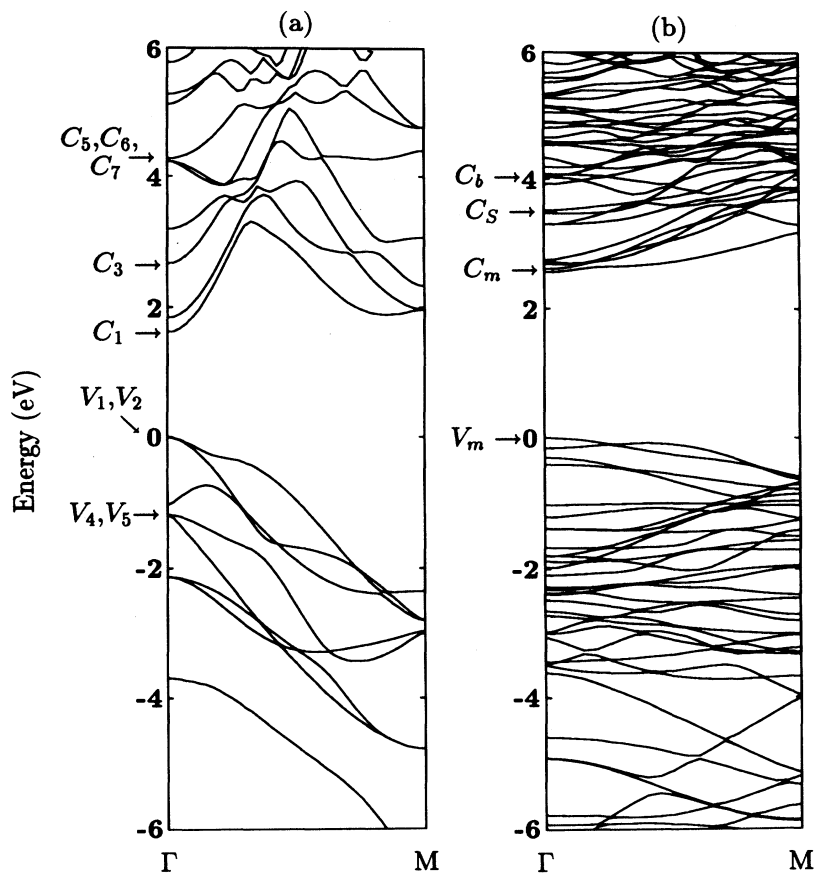


FIG. 2. The band structures for the five-layer quantum well (a) and  $5 \times 5$  quantum wire (b). The  $M$  points correspond to the unfolded  $X$  points in the Brillouin zone of bulk Si.

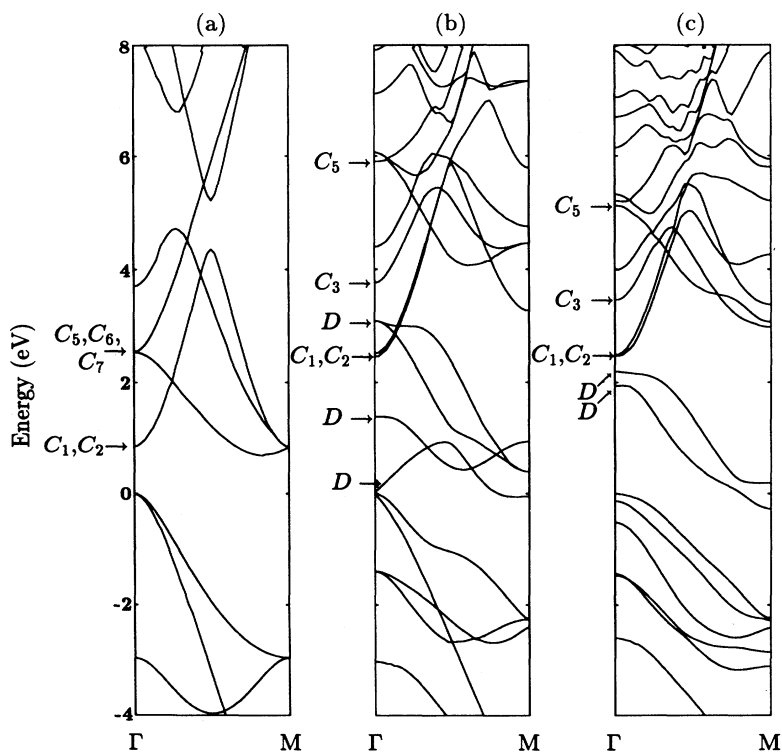


FIG. 3. The band structures for crystalline Si (a) and the five-layer quantum well (b) and (c). In (b), the dangling bonds on the surfaces are nonpassivated by hydrogen, while in (c) a half of the dangling bonds are passivated. The dangling bond states are denoted by  $D$  in (b) and (c).

TABLE I. Oscillator strengths  $f_{cv}$  for various interband transitions at the  $\Gamma$  point in the five-layer quantum well and the  $5\times 5$  quantum wire. The polarization direction is chosen to be parallel to the plane of the quantum well and the wire orientation. The  $V_1$  and  $V_2$  states are generated as well as the  $V_4$  and  $V_5$  states.

System	Valence states		Conduction states	$\Delta E_{cv}$ (eV)	$f_{cv}$
Five-layer quantum well	$V_1, V_2$	$\rightarrow$	$C_1$	1.63	0.000
		$\rightarrow$	$C_3$	2.67	2.640
		$\rightarrow$	$C_5$	4.23	0.000
	$V_3$	$\rightarrow$	$C_1$	2.68	0.000
		$\rightarrow$	$C_3$	3.72	0.000
		$\rightarrow$	$C_5$	5.29	0.221
	$V_4, V_5$	$\rightarrow$	$C_1$	2.81	1.395
		$\rightarrow$	$C_3$	3.85	1.052
		$\rightarrow$	$C_5$	5.42	0.000
$5\times 5$ quantum wire	$V_m$	$\rightarrow$	$C_m$	2.61	0.000
		$\rightarrow$	$C_s$	3.50	1.005
		$\rightarrow$	$C_b$	4.03	1.011
	$V_4$	$\rightarrow$	$C_m$	2.92	1.255
		$\rightarrow$	$C_s$	3.80	0.000
		$\rightarrow$	$C_b$	4.34	0.000

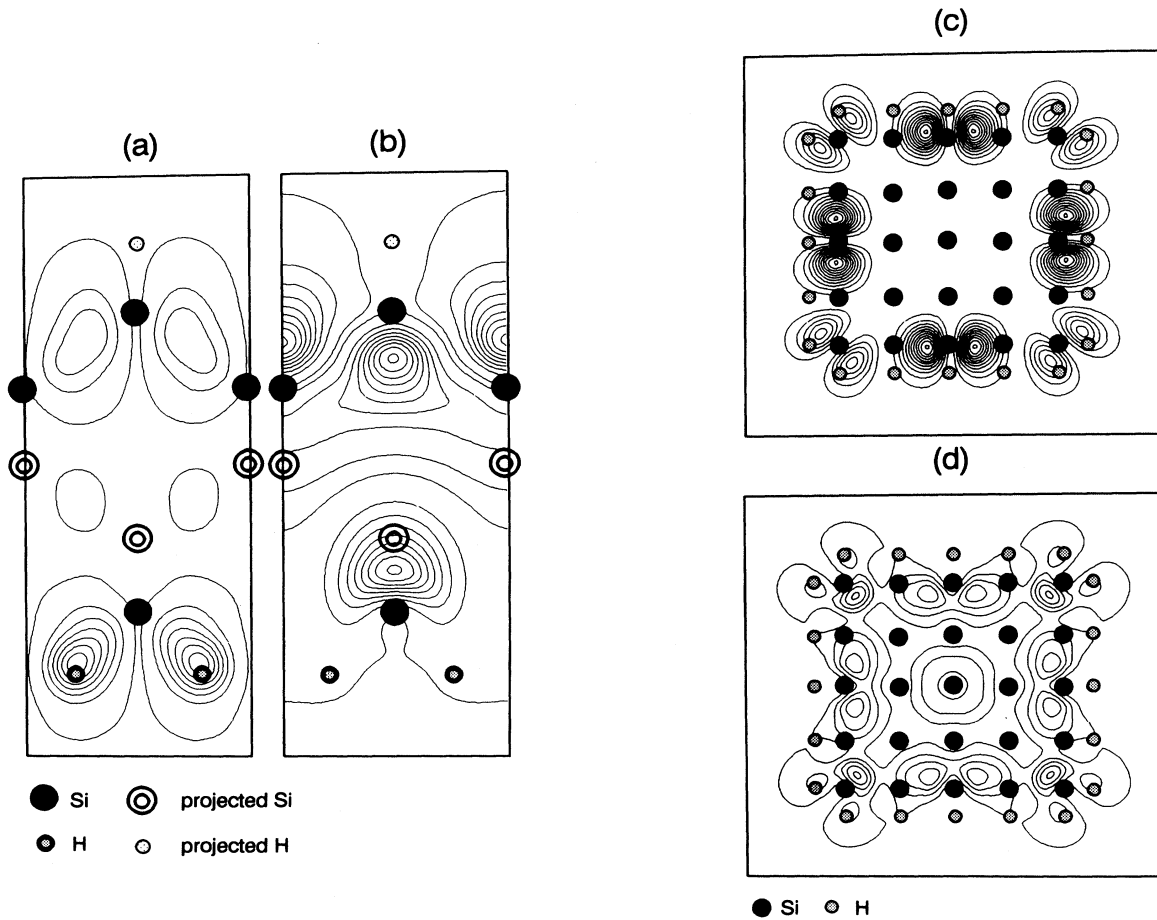


FIG. 4. The electron charge densities are plotted for the (a)  $V_1$  and (b)  $C_3$  states in the five-layer quantum well and for the (c)  $V_m$  and (d)  $C_s$  states in the  $5\times 5$  quantum wire. The charge density for the  $V_4$  state is found to be similar to that of the  $V_1$  state.

of the Si-H bonds, with some charges between the top- and sub-layer Si atoms. Since the  $V_1$  state is significantly overlapped with the  $C_3$  conduction band state near the surface region, the optical transition between these states is considerable. Similarly, the  $V_m$  VBM state in the quantum wire is derived from the interactions between the H and surface Si atoms; thus the optical transition from the  $V_m$  state to the confined  $C_s$  state shows strong oscillator strength.

By calculating the imaginary part of the dielectric function  $\epsilon_2(\omega)$ , we are able to obtain information directly on photoluminescence excitation spectroscopy. The calculated  $\epsilon_2(\omega)$ 's for the quantum well and wires are drawn in Fig. 5. In the quantum well,  $\epsilon_2(\omega)$  shows rapidly increasing behavior near 4 eV, independent of the polarization direction. Such an increase in  $\epsilon_2$  is similar to that of  $c$ -Si as shown in Fig. 5 and is associated with the

bulklike optical transitions between parallel bands along the  $\Gamma$ - $L$  axis in the BZ of bulk Si. However, for energies below 4 eV, the optical response strongly depends on the polarization direction, giving rise to anisotropic optical transitions. Similar results were also found in other calculations.<sup>6,7</sup> In the optical energy region, we find a very strong optical response, which is absent in  $c$ -Si, when the polarization direction is parallel to the plane of the quantum well. This increase of the optical absorption is mostly attributed to the transitions from the  $V_1$  to the confined  $C_3$  state and from the  $V_4$  to the  $C_1$  and  $C_3$  states. In the quantum wires, we also find similar behavior in the dielectric functions as shown in Fig. 5. The bulklike dielectric response appears at energies above 4 eV, which is the energy separation between the parallel bands on the  $\Gamma$ - $L$  axis. The different threshold energies of the bulklike excitations in the two quantum wires result from the different sizes of the wires. For energies below the threshold energy, both the  $5 \times 5$  and  $7 \times 7$  quantum wires show prominent optical peaks, similar to the quantum well. In this case, we find strong dielectric responses when the polarization direction is parallel to the quantum wire, while the response functions are significantly reduced for the polarization perpendicular to the wire. In the  $5 \times 5$  quantum wire,  $\epsilon_2$  has two peaks at energies of 3 and 4 eV in the optical region, while they occur at 2.6 and 3.6 eV in the  $7 \times 7$  wire. The lower energy peak is attributed to the  $V_4$ - $C_m$  transition; however, its intensity is much weakened, as compared to the higher energy peak which is mostly derived from the  $V_m$ - $C_s$  transition. Because of the considerable confinement effect in the wire structure, the energy bands are flattened more significantly; thus the optical response due to the confined states is more prominent than in the quantum well. We point out that although our results are similar to previous theoretical calculations,<sup>7</sup> the interpretation of the optical peaks was not given properly. Since in the previous work the dielectric functions were calculated only for energies up to 3.5 eV, the bulklike excitations were not properly seen in the response function. Only the lower energy peak found in our calculations was attributed to the quantum wire effect, while the higher energy peak was interpreted as the bulklike excitation in the previous calculation.<sup>7</sup> However, our results indicate that the second peak in the luminescence excitation spectroscopy is indeed a wire-related feature, while the bulklike excitations occur at a few tenths of an eV higher energies than the wire-related peak.

We examine the effect of hydrogenated surfaces on the absorption spectra by calculating the dielectric functions for the five-layer quantum wells with surfaces partially passivated and nonpassivated by hydrogen and compare the results with that of the fully passivated quantum well in Fig. 6. When H atoms are partially or completely removed from the surfaces, the contributions from the  $V_1$  and  $V_4$  states to the optical transition are reduced because these states are associated with the Si-H bonds. In fact, we find such a decrease of the H-related states in the local density of states (LDOS), which provides information on the contribution of each atom to a given energy state.<sup>23</sup>

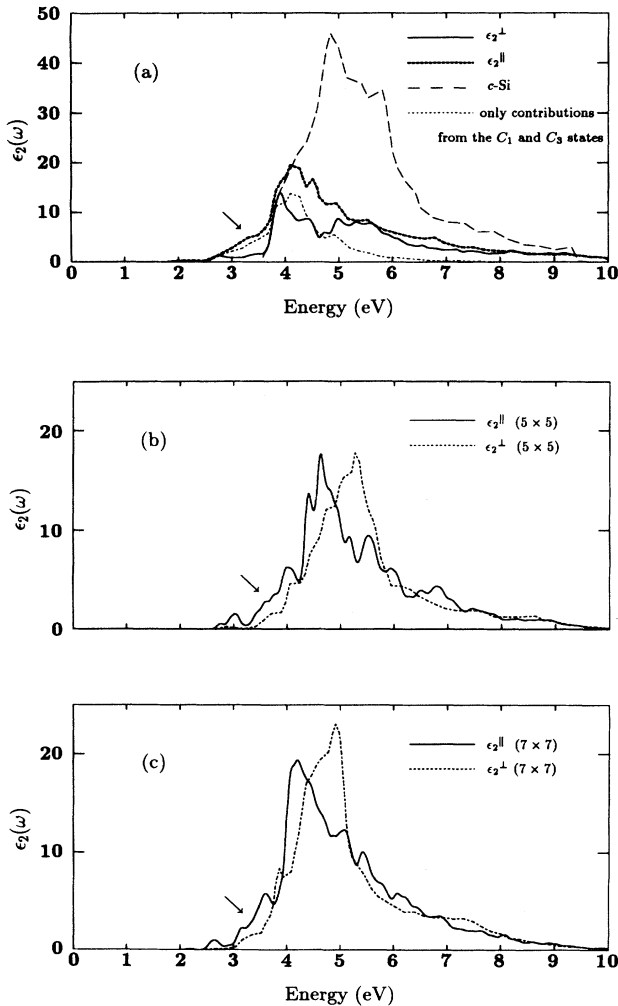


FIG. 5. The imaginary parts of the dielectric functions ( $\epsilon_2$ ) are plotted as a function of energy for different polarization directions in the five-layer quantum well (a) and  $5 \times 5$  and  $7 \times 7$  quantum wires (b) and (c). In (a),  $\epsilon_2$  for  $c$ -Si is shifted by 0.8 eV and compared with that obtained from only the optical transitions to the  $C_1$  and  $C_3$  conduction states.

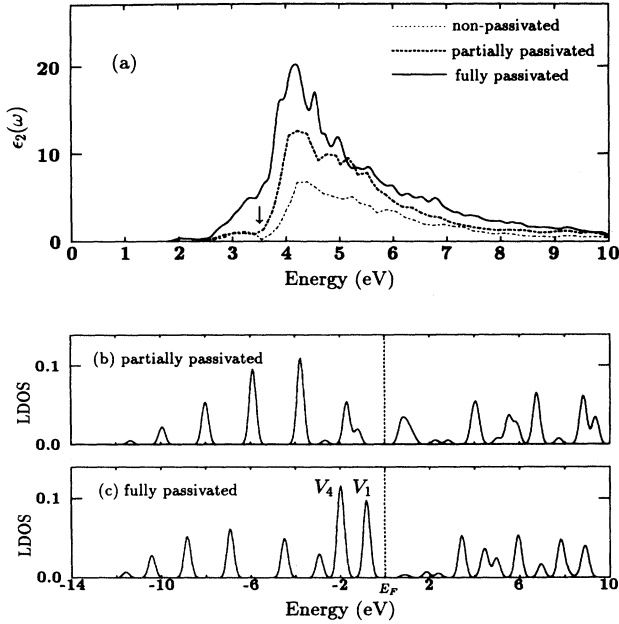


FIG. 6. In (a),  $\epsilon_2$  of the five-layer quantum well with the surfaces fully passivated by hydrogen is compared with those for the partially passivated and nonpassivated quantum wells. The local densities of states calculated at the  $\Gamma$  point are plotted for the partially passivated (b) and fully passivated (c) quantum wells.

$$D(E, \tau) = 2 \sum_{n, \mathbf{k}} \delta(E - E_{n, \mathbf{k}}) \int_{\Omega} |\psi_{n, \mathbf{k}}(\mathbf{r} - \tau)|^2 d^3r, \quad (3)$$

where  $\tau$  denotes an atomic position. When the hydrogenation on the surfaces is decreased, the H-related  $V_1$  and  $V_4$  states near the VBM are much reduced and the enhancement of  $\epsilon_2$  in the energy range 2.6 – 3.6 eV disappears, as shown in Fig. 6, except for very weak peaks due to dangling bonds which are not plotted here. This result supports experimental findings that the degradation of photoluminescence intensity from porous Si is accompanied by the reduction of H-related vibrational modes,<sup>13–15</sup> implying that the Si-H bonds noticeably affect luminescence.

Since the radiative luminescence process involves impurity scattering and the recombination of excitonic states formed from band-edge states, a direct comparison of  $\epsilon_2(\omega)$  with luminescence spectroscopy cannot be made. Thus we compare our calculated band-edge exci-

tation peaks for the quantum wires with measured photoluminescence excitation spectra. Since the sizes of the quantum wires considered here are smaller than those found experimentally in porous Si,<sup>1</sup> our calculated energy gaps are generally higher because the energy gap increases as the quantum size decreases (see Table II). The calculated energy gaps of quantum wires are fitted with a term in  $1/d^2$ , where  $d$  is the side length of a quantum wire. Because the local-density functional approximation is used, the energy gaps are underestimated by about 0.4 eV. With the LDA band-gap correction, we estimate the optical peak energy which appears weakly near the band gap in  $\epsilon_2(\omega)$  to be 1.9 – 2.1 eV for the sizes  $d = 20 - 35$  Å, assuming that the energy gap approaches 1.17 eV in the limit  $d \rightarrow \infty$ , i.e., in c-Si. These results are consistent with previous theoretical calculations<sup>7</sup> and also in good agreement with the optical absorption spectra observed at 2.1–2.4 eV in porous Si with crystallite diameters in the range 20–35 Å.<sup>24</sup> However, the positions of the wire-related main peaks in  $\epsilon_2(\omega)$  are estimated to be 2.9–3.1 eV for the sizes  $d = 20-35$  Å, which are higher by about 1 eV than the measured absorption peaks. In quantum systems, electron and hole pairs contributing to radiative recombination are localized in confined regions; thus the binding energy of an exciton is quite high and estimated to be about 0.4 eV for quantum sizes ranging from 20 to 50 Å.<sup>6</sup> If the exciton binding effect is included, our band-edge absorption peaks will be located at 1.5 – 1.7 eV, which is compatible with the observed photoluminescence spectra at energies of 1.4 – 1.7 eV.<sup>1,14,15</sup> From this result, we suggest that the visible luminescence from porous Si occurs near the surface region and is attributed to the optical transitions between some localized states which are caused by quantum confinement and strong interactions between hydrogen and surface Si atoms. Finally, since there is no conclusive evidence that siloxene does not exist in porous Si, further theoretical studies are required to investigate the role of siloxene at surfaces.

In conclusion, we have studied the optical properties of several confined Si systems by calculating the dielectric response function and found prominent absorption peaks in the range of visible light. In the quantum wires, the imaginary part of the dielectric function shows luminescence excitation peaks near the band-gap energy, and the peak positions are in good agreement with measured absorption spectra. Strong wire-related absorption peaks are also found at energies away from the band gap; however, these peaks were interpreted as bulklike excitations in previous work. The wire-related excitation spectra are attributed to the enhancement of optical transitions between localized states in the near-surface region which

TABLE II. The calculated LDA band gaps and the side and major optical peaks in  $\epsilon_2$  are given.

	Well (nine layers)	Well (five layers)	Wire (7×7)	Wire (5×5)
Size (Å)	10.86	5.43	11.52	7.68
LDA band gap (eV)	1.14	1.63	1.93	2.55
Side optical peak in $\epsilon_2$ (eV)			2.6	3.0
Main optical peak in $\epsilon_2$ (eV)			3.6	4.0

are caused by quantum confinement and hydrogenation effects. Both the Si quantum wells and wires considered here exhibit a direct gap, while the band gap of crystalline Si is indirect, enhancing the oscillator strength of the direct optical transitions. Thus our results for the electronic structure and the absorption spectra support the previous idea that the concentration of H or SiH<sub>2</sub> in

the near-surface region and the size of porous Si crystallites are important for radiative photoluminescence in porous Si.

This work was supported by the CMS at KAIST and the SPRC at Jeonbuk National University.

- 
- <sup>1</sup> L. T. Canham, *Appl. Phys. Lett.* **57**, 1046 (1990); A. G. Cullis and L. T. Canham, *Nature* **353**, 335 (1991).
- <sup>2</sup> V. Lehmann and U. Gösele, *Appl. Phys. Lett.* **58**, 856 (1991); S. Gardelis, J. S. Rimmer, P. Dawson, B. Hamilton, R. A. Kubiak, T. E. Whall, and E. H. C. Parker, *ibid.* **59**, 2118 (1991).
- <sup>3</sup> J. C. Vial, A. Bsiesy, F. Gaspard, R. Hérino, M. Ligeon, F. Muller, R. Romestain, and R. M. Macfarlane, *Phys. Rev. B* **45**, 14 171 (1992).
- <sup>4</sup> J. Wang, H.-B. Jiang, W.-C. Wang, J.-B. Zheng, F.-L. Zhang, P.-H. Hao, X.-Y. Hou, and X. Wang, *Phys. Rev. Lett.* **69**, 3252 (1992).
- <sup>5</sup> S.-L. Zhang, K.-S. Ho, Y. Hou, B. Qian, P. Diao, and S. Cai, *Appl. Phys. Lett.* **62**, 642 (1993).
- <sup>6</sup> T. Ohno, K. Shiraishi, and T. Ogawa, *Phys. Rev. Lett.* **69**, 2400 (1992), and references therein.
- <sup>7</sup> F. Buda, J. Kohanoff, and M. Parrinello, *Phys. Rev. Lett.* **69**, 1272 (1992).
- <sup>8</sup> A. J. Read, R. J. Needs, K. J. Nash, L. T. Canham, P. D. J. Calcott, and A. Qteish, *Phys. Rev. Lett.* **69**, 1232 (1992).
- <sup>9</sup> C. G. Van de Walle and J. E. Northrup, *Phys. Rev. Lett.* **70**, 1116 (1993).
- <sup>10</sup> P. Deák, M. Rosenbauer, M. Stutzmann, J. Weber, and M. S. Brandt, *Phys. Rev. Lett.* **69**, 2531 (1992); M. Stutzmann, M. S. Brandt, M. Rosenbauer, J. Weber, and H. D. Fuchs, *Phys. Rev. B* **47**, 4806 (1993).
- <sup>11</sup> M. A. Tischler, R. T. Collins, J. H. Stathis, and J. C. Tsang, *Appl. Phys. Lett.* **60**, 639 (1992).
- <sup>12</sup> Z. Y. Xu, M. Gal, and M. Gross, *Appl. Phys. Lett.* **60**, 1375 (1992).
- <sup>13</sup> C. Tsai, K.-H. Li, D. S. Kinosky, R.-Z. Qian, T.-C. Hsu, J. T. Irby, S. K. Banerjee, A. F. Tasch, J. C. Campbell, B. K. Hance, and J. M. White, *Appl. Phys. Lett.* **60**, 1700 (1992).
- <sup>14</sup> S. M. Prokes, O. J. Glembocki, V. M. Bermudez, R. Kaplan, L. E. Friedersdorf, and P. C. Searson, *Phys. Rev. B* **45**, 13 788 (1992).
- <sup>15</sup> Y. M. Weng, Zh. N. Fan, and X. F. Zong, *Appl. Phys. Lett.* **63**, 168 (1993).
- <sup>16</sup> J. Ihm, A. Zunger, and M. L. Cohen, *J. Phys. C* **12**, 4409 (1979).
- <sup>17</sup> W. Kohn and L. J. Sham, *Phys. Rev.* **140**, A1133 (1965).
- <sup>18</sup> E. Wigner, *Trans. Faraday Soc.* **34**, 678 (1938).
- <sup>19</sup> N. Troullier and J. L. Martins, *Phys. Rev. B* **43**, 1993 (1991).
- <sup>20</sup> L. Kleinman and D. M. Bylander, *Phys. Rev. Lett.* **48**, 1425 (1982).
- <sup>21</sup> C. H. Park, I.-H. Lee, and K. J. Chang, *Phys. Rev. B* **47**, 15 996 (1993).
- <sup>22</sup> J. Rath and A. J. Freeman, *Phys. Rev. B* **11**, 2109 (1975).
- <sup>23</sup> C. T. Chan and S. G. Louie, *Phys. Rev. B* **27**, 3325 (1983).
- <sup>24</sup> Y. Kanemitsu, H. Uto, Y. Masumoto, T. Matsumoto, T. Futagi, and H. Mimura, *Phys. Rev. B* **48**, 2827 (1993).

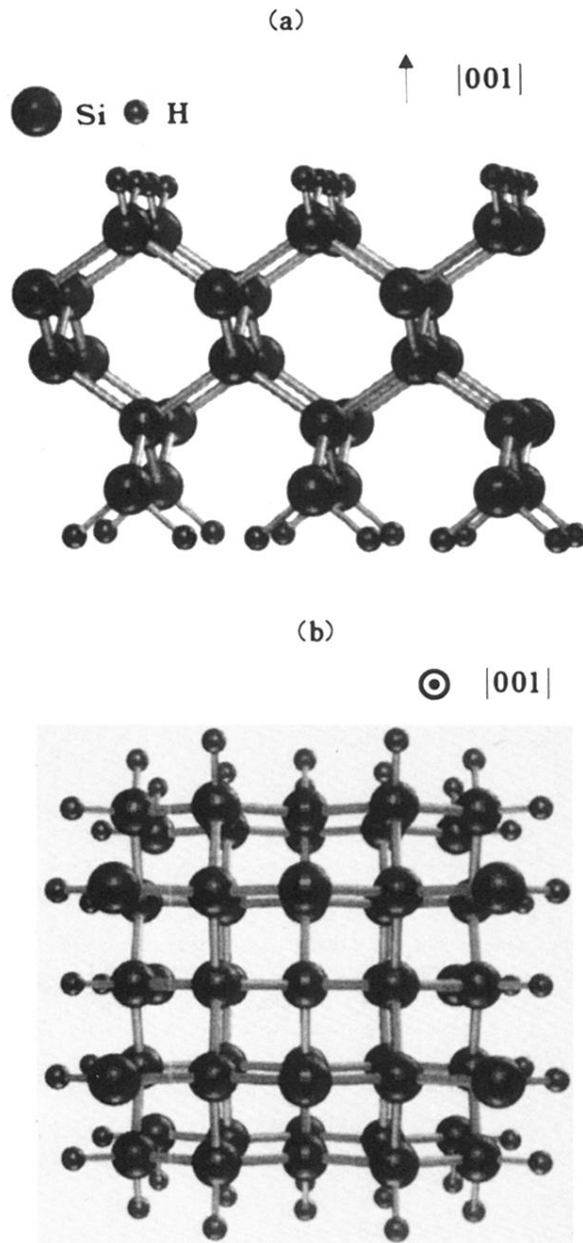


FIG. 1. Ball and stick models for the five-layer quantum well (a) and  $5 \times 5$  quantum wire (b). The unit cell of the quantum well includes five Si and four H atoms and is repeated on the (001) plane. The wire is chosen along the [001] direction with the unit cell containing 25 Si and 20 H atoms.